

## ***Helmichia glandulicola* sp.nov. (Microspora, Thelohaniidae): morphology, development and influence on salivary glands of *Chironomus anthracinus* (Diptera, Chironomidae)\***

Wolfgang F. Wülker<sup>1</sup> and Jaroslav Weiser<sup>2</sup>

<sup>1</sup> Institut für Biologie I (Zoologie), der Universität, Albertstr. 21 a, W-7800 Freiburg, Federal Republic of Germany

<sup>2</sup> Institute of Entomology, Academy of Sciences, Branišovská 31, 37005 České Budějovice, Czechoslovakia

Accepted December 15, 1990

**Abstract.** *Helmichia glandulicola*, a microsporidian parasite specific for cells of the salivary glands of the midge *Chironomus anthracinus*, is described. It is characterized by tubular spores with a distinct polar cap that are enclosed in persistent octosporous pansporoblasts. The pansporoblastic membrane is formed early during the first sporogonial division. A granular secretion occurs in the pansporoblast among the oval sporoblasts, which subsequently become tubular and display a rigid polar filament. The solitary infected cell reacts with hypertrophy and depletion of its endoplasmic reticulum and ribosomal system. There are differences in the morphology of mitochondria in infected vs noninfected cells. The production of saliva by the host is only partially reduced following infection.

Among the microsporidia that infect larvae of chironomid midges, a very specific role is played by a species which infects the salivary glands. This infection was first recorded by Keyl (1960, 1963) in larvae of *Chironomus anthracinus* Zetterstedt, in which the infected cells of the gland had become hypertrophic, protruding from the surface of the gland. These cells contained large numbers of rod-shaped spores. In hypertrophic cells the polytene chromosomes in increased nuclei were significantly enlarged and a large chromatin mass resulted from an additional 3- to 5-fold replication (Keyl 1960). The impacts of this microsporidian infection on the cytoplasm of infected glandular cells and on the function of the latter in the secretion of saliva were not known at that time. Keyl (1960) has suggested that the infected cell contributes little or nothing to saliva production. On an ultramicroscopic basis, the present report describes in detail some changes induced by this microsporidian in the cytoplasm of *C. anthracinus*. A preliminary

report of part of the results has been published by Wülker (1987). In addition, the ultrastructural examination of different developmental stages of the parasite enabled its description as a new species on the basis of comparisons with paratype material and descriptions of *H. aggregata* (Larsson 1982). Our results are comparable with those previously obtained on cytoplasmic changes in salivary glands of *Sciara* following their infection with the microsporidian *Thelohania* (Jurand et al. 1967).

### **Materials and methods**

The material studied was collected on July 19 and 28, 1985, from the mud of the bottom of Apeltunvatnet near Bergen, Norway. In this small, shallow lake, *Chironomus anthracinus* occurs together with *C. plumosus* and another unidentified *Chironomus* species. Third- and fourth-instar larvae were present at the time of sample collection. The infection was apparent as minute white spots on salivary glands in the transparent body of the larvae, which were dissected at the Institute of Zoology, University of Bergen. One part of the glandulae was used for the preparation of smears, which were fixed in methanol and stained with Giemsa's stain. Another part was fixed according to the method of Karnovsky (1965), then refixed in OsO<sub>4</sub> and prepared for embedding. A second set of living larvae were transported in mud to the Freiburg laboratory, where they were dissected. Infected glands were fixed in 6% glutaraldehyde in cacodylate buffer and refixed in OsO<sub>4</sub>. All material was embedded in Epon following dehydration in an alcohol gradient. Sections were cut using a Reichert Om O2 ultramicrotome; 1-µm sections were stained with toluidine blue and examined with a Zeiss photomicroscope, and ultrathin sections were stained with uranyl acetate and lead citrate and analysed using a Zeiss U9A ultramicroscope.

### **Results and discussion**

#### *The pathogen*

**Light microscopy.** Nearly 20% of about 600 investigated larvae of *Chironomus anthracinus* were infected; other *Chironomus* species collected from the lake were not infected. The infection was limited to the salivary glands,

\* Dedicated to Prof. Dr. J. Eckert (Zürich) on the occasion of his 60th birthday

Offprint requests to: W. Wülker

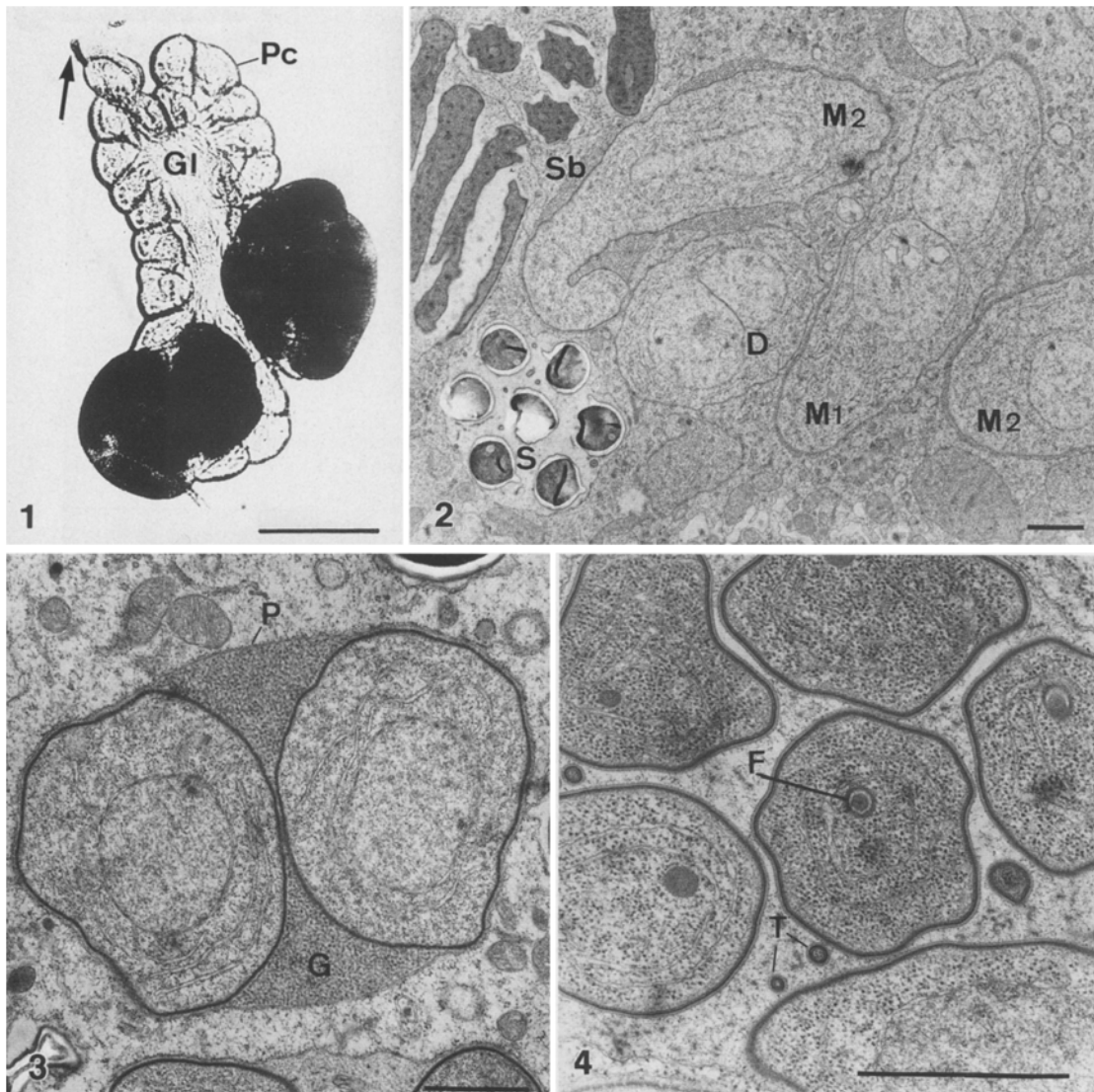


**Fig. 1.** Salivary gland of *Chironomus anthracinus*, beginning of the 4th larval instar, showing two hypertrophic cells infected with *Helmichia glandulicola* (opaque). *Pc*, large polytenic cells; *Gl*, gland lumen (filled with saliva), arrow, salivary duct. Photograph by I. Wildelau. Bar = 250  $\mu$ m

**Fig. 2.** Ultrathin section of an infected cell, showing merogonial stages. *M1* = young merozoite without a pansporoblastic membrane or granular secretions (two nuclei not yet adhering can be seen in the median plane). *M2*, late merozoites within a pansporoblastic membrane, with granules filling the space inside the membrane; *D*, diplocaryon stage; *S*, spores in a pansporoblast (cross section); *Sb*, pansporoblast with sporoblasts. Bar = 1  $\mu$ m

**Fig. 3.** First sporogonial division. The sporoblast membrane is thin and the space inside the pansporoblastic membrane (sporophorous vesicle) is filled with granula. *G*, granules, *P*, pansporoblastic membrane. Bar = 1  $\mu$ m

**Fig. 4.** Sporoblast after the third division resulting in eight single sporoblasts in a sporophorous vesicle. One cross section is shown of the polar filament (*F*) in each. The number of granula is reduced, note the 6 cross sections of tubular secretions (*T*). Bar = 1  $\mu$ m

and in most animals it involved only a few of the "large polytenic cells" (sensu Jacob and Jurand 1965; see Fig. 1). The parasitized cells were preferably situated near the blunt end of the gland, far away from the salivary duct. The saliva inside the gland and salivary duct did not contain any spores. The infection did not spread from infected hypertrophic cells to the adjoining non-hypertrophic cells. There was no evidence of any infection with *Helmichia* in tissues other than the salivary gland, including the fat body of the larvae.

Infected tissues in stained smears were filled with a foamy structure comprising empty spherical vacuoles measuring 10–12  $\mu$ m in diameter and with bundles of spores in groups of eight. On the thin periphery of the smear inside the foamy vacuoles, details of sporogonial stages, usually consisting of eight uninucleate sporoblasts, showed faint staining and the vacuole represented the interior of the pansporoblastic membrane. The spores were tubular, 3–4  $\times$  1.2–1.5  $\mu$ m, and Giemsa staining revealed a typical polar cap on the anterior pole

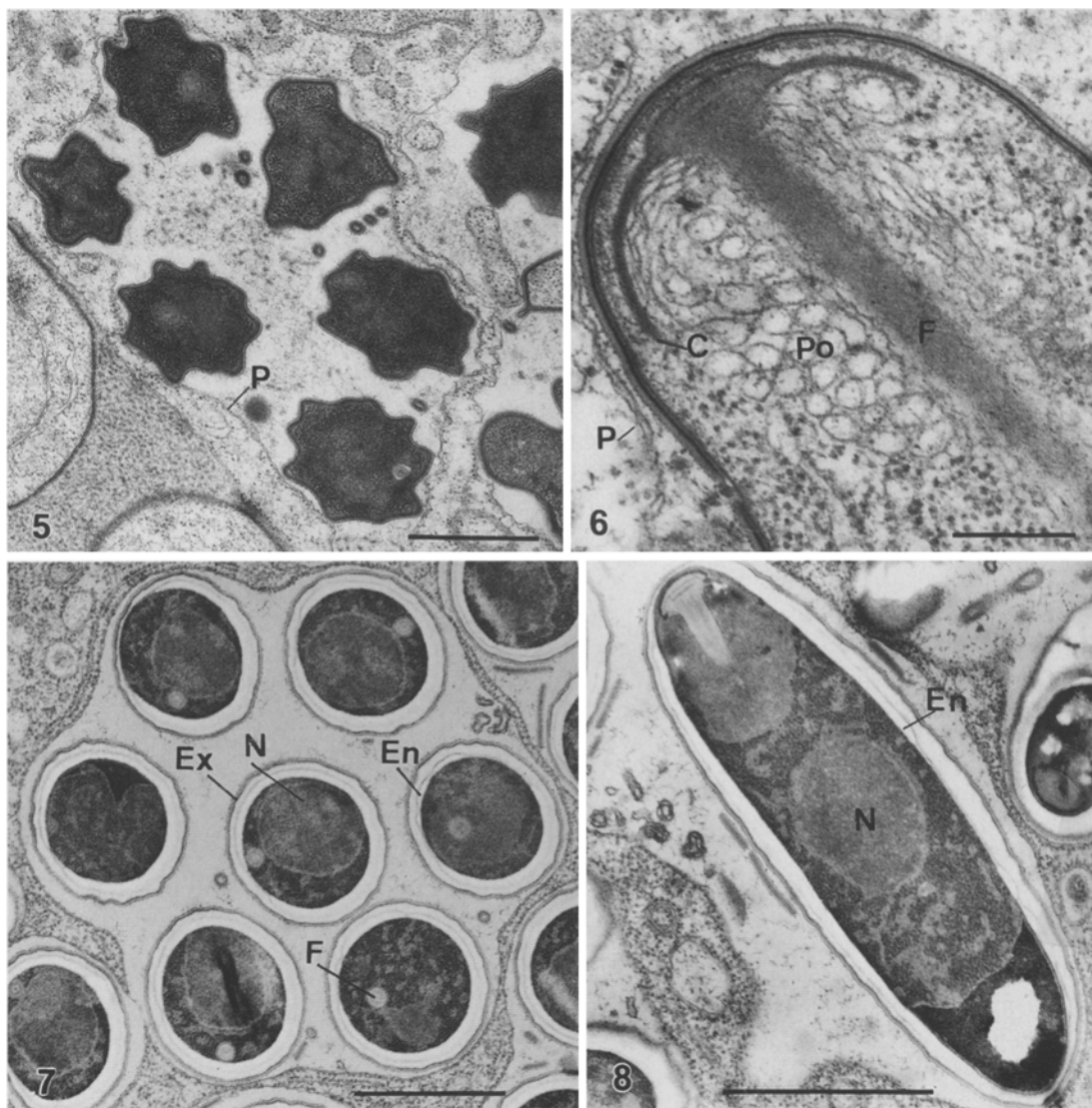


**Fig. 5.** Late sporoblasts with a thin "cemented" membrane. The pansporoblastic membrane (*P*) thin, in its interior are remains of granular and tubular secretions. *Bar* = 1  $\mu$ m

**Fig. 6.** Anterior end of the young spore, showing the fixing disc of the polar filament (*F*) and the polar cap (*C*). In the spore wall, the exospore and endospore are sticking together without secretion of the chitinous layer of the endospore. A polaroplast (*Po*) is shown in its tubular phase of development. On the left side, the pansporoblastic membrane (*P*) appears as a double membrane with many interconnections. *Bar* = 0.25  $\mu$ m

**Fig. 7.** Cross sections of 7 of the 8 spores in the pansporoplast, showing the thin exospore (*Ex*) and the thick endospore (*En*). In the spore's interior, a cross section of the polar tube (*F*) and the nucleus (*N*) can be seen; the sporophorous vesicle has a thin wall. *Bar* = 1  $\mu$ m

**Fig. 8.** Longitudinal section of a mature spore, showing polar attenuation of the endospore (*En*) and the fixing disc of the polar tube. The nucleus (*N*) can be seen in the center and the remains of the posterosome, in the posterior portion. *Bar* = 1  $\mu$ m

of the spore; the spore content was grouped in two or three indefinite clumps in the centre and the posterior part. The anterior vacuole typical of microsporidian spores was not observed. On smears we could not find any indication of the release of polar filament attributable to its activation during drying of the smear.

Broad oval to spherical vegetative stages were often seen in groups. Late merozoites had a single, rather broad nucleus. Later, oval binucleate stages showing two nuclei adhering medially in a broad contact zone, i.e. typical diplokarya, were formed; their nuclei were enlarged and their cytoplasm was reduced. Next in devel-

opment were uninucleate stages with yet enlarged nuclei, which apparently began sporogony and divided into two, four and then eight sporonts that were all enclosed in a common membrane originating from the membrane of the sporont that had separated during the first division. All further divisions resulted in single, uninucleate stages that were not connected to a central part by plasmatic bridges.

Inside the pansporoblastic space, some stained granules remained until the spores had reached maturation. At the stage of eight sporoblasts, the granules disappeared and the sporoblasts filled only a minor part of

the spherical empty space that corresponds with the foamy structures in the dense cytoplasm of the host cell. Young sporoblasts are broadly oval to navicular and were clustered on the wall in one part of the pansporoblast. Details in their interior were poorly stained and the nuclei of some sporoblasts contained mitotic figures.

**Electron microscopy.** On ultrathin sections the earliest stages were late merozoites (Fig. 2), which formed spherical cells with a rather large nucleus that evidently contained meiotic chromosomes and synaptonemal complexes, analogous to stages in the genera *Amblyospora* and *Parathelohania*. In the next step the large nuclei adhered together in a median plane typical of diplokarya (Fig. 2). The surface membrane of these stages persisted throughout sporogony; it was not very prominent in sections, but it delimited the space within the pansporoblast very efficiently throughout the maturation process, reaching its final diameter (10–12 µm) very rapidly. The pansporoblastic membrane did not adhere tightly to the developmental stages.

In the next step, in which two uninucleate sporonts were formed (Fig. 3), a fine mass of secretion granules appeared in the space around the sporonts. These stages measure  $5\text{--}7 \times 10\text{--}12$  µm; their cytoplasm contained numerous electron-dense granules and long membranes of endoplasmic reticulum encircled the central nucleus. At the next divisions, which followed synchronously, the outer membrane surrounded the subsequent stages. A periparasitic vacuole was formed by the host cell around the pansporoblastic membrane, and in most cases it adhered firmly to the wall of the pansporoblast. The granular secretion was present during the first two divisions, but with the formation of eight sporoblasts and spores the granules were dissolved, leaving only a more resistant tubular secretion that was visible in cross sections of late pansporoblasts (Figs. 4, 5). The wall of the sporoblasts underwent the usual period of thickening and "cementation", resulting in loss of permeability for fixatives and stains. The first indications of the formation of a polar filament appeared early in octosporoblastic pansporoblasts, which were broad and oval and measured  $2\text{--}2.5 \times 3\text{--}4$  µm in diameter (Fig. 4).

Mature spores had a thin, distinct, electron-dense exospore and a thick, translucent endospore (Figs. 7, 8) that attenuated in the apical pole, where the polar cap adheres from the interior to the globular pole (Fig. 8). The anchoring disc (Figs. 6, 8, 9) protruded apically over the polar cap and the polar filament, which measured  $2.8\text{--}3$  µm in length and  $0.2$  µm in diameter, extended from the centre of the spore to its posterior end. The polar filament is straight, being of equal thickness and structure over its whole length, and ends bluntly. Throughout its development, it does not coil and seems to be rigid, reminiscent of the manubrium that appears in spores of Mrazekiidae. The polaroplast was lamellar in mature spores, with the lamellae adhering to the filament (Fig. 9); in young spores, tubular structures were interposed between the lamellae (Fig. 6). The spore was filled with the germ containing dense masses of ribo-

somes and lamellae of the endoplasmic reticulum. The single nucleus (Fig. 8) laid in the second third of the spore, was spherical and was not compressed by the filament. The posterior pole contained the remains of the posterosome (Golgi).

**Diagnosis.** The parasite described herein showed the characteristics of the genus *Helmichia*, established by Larsson in 1982. Using a paratype slide, provided by courtesy of Dr. Larsson, we compared it with *Helmichia aggregata*. The sporogonic development of our parasite differed from that of *H. aggregata* in the early formation of the pansporoblastic membrane from the first sporogonial division, in the dense granular deposit filling the space around the sporoblasts in the pansporoblast and in the absence of the massive tubular secretion observed in *H. aggregata* by Larsson. *H. aggregata* sporoblasts that had been cut transversally were not flat discs, but rather appeared oval or spherical in shape.

Our microsporidian was specifically localized in the tissues of its host and seemed to be host-specific in that it did not infect other chironomid species collected from the same lake. The characteristics of our parasites seemed identical with those of material described by Keyl (1960) in the same host. In contrast, the infection with *H. aggregata* was concentrated in the fat body of *Endochironomus* larvae only. We believe that the described microsporidian differs from *H. aggregata* in many important details and we propose that the microsporidian found in the salivary gland of *Chironomus anthracinus* be given the name *Helmichia glandulicola* sp.nov. The holotype is deposited in the collection of J. Weiser, and paratypes in the collection of W. Wülker.

#### *Interaction with the host*

In studies of the distribution of *Vairimorpha plodiae* in the wax moth, David (1991) demonstrated that lymphocytes with phagocytized microsporidian spores adhere to silk glands of the caterpillar and introduce the infection into cells of this tissue; the parasite does not enter the organ via its outlet channel. The same situation seemed to apply to the infection of *Chironomus* salivary glands. The parasite grew in the non-secretory base of the cell, and the abnormal growth manifested in the expansion of this part of the cell beyond of the surface of the gland.

The ultrastructure of normal salivary glands of the chironomids *Smittia* and *Chironomus* is well known (Jacob and Jurand 1965; Kloetzel and Laufer 1969). Our ultramicroscopy studies raised some considerations as to how this structure changes after parasitization and whether or not saliva is secreted by the infected cell. Mitochondria in infected cells are more numerous, and are thus generally smaller than those in non-infected cells. Figure 10 illustrates an apparently extreme situation in two adjacent cells. The mitochondria in the infected cell are well formed, showing distinct staining and dense cristae. In the non-infected cell on the right mito-

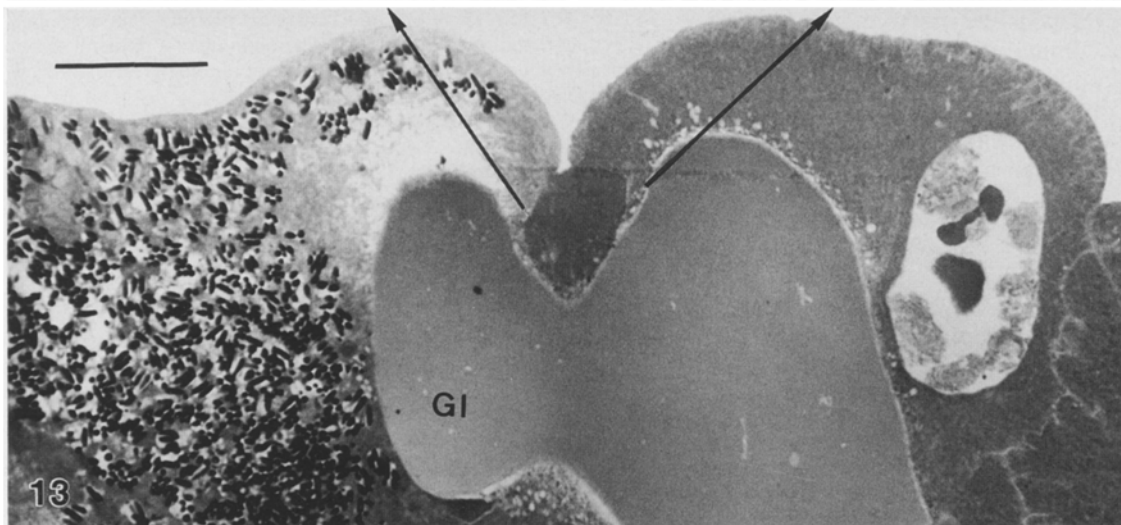
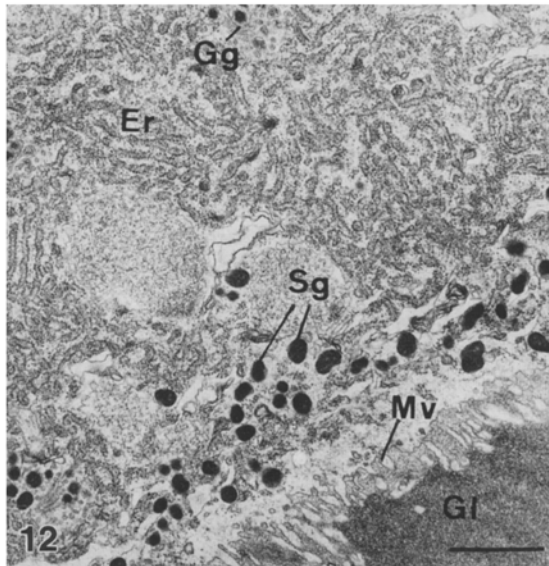
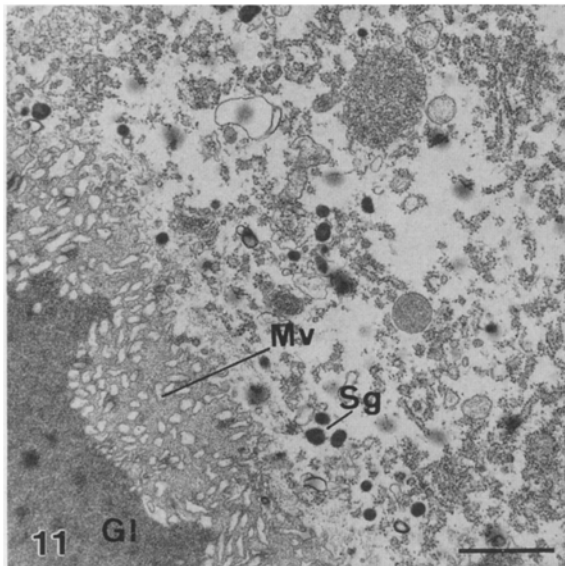
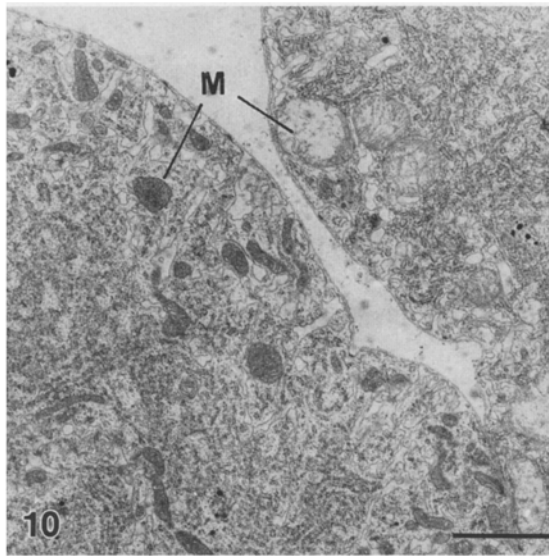
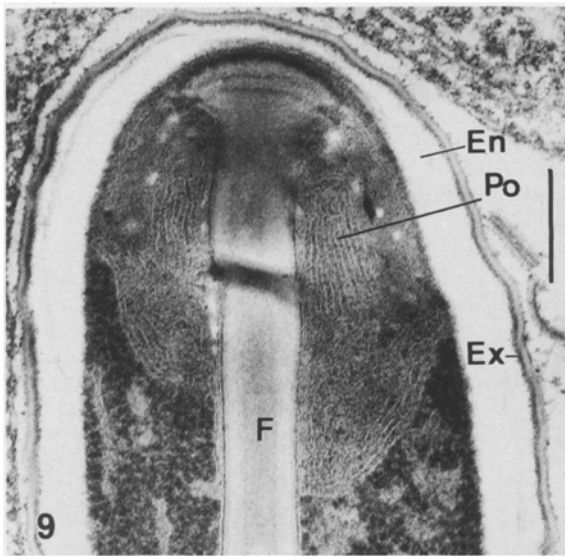


**Fig. 9.** Anterior pole of a mature spore showing the fixing disc of the polar tube, the polar filament (*F*), the lamellar polaroplast (*Po*) and the endospore (*En*) and exospore (*Ex*) of the spore wall. *Bar* = 0.25  $\mu$ m

**Fig. 10.** Two adjacent cells of the gland. *Left*: infected cell, *right*: uninfected cell. Note the differences in mitochondria (*M*) and ER. *Bar* = 2  $\mu$ m

**Figs. 11, 12.** Cytoplasmic structures in the infected (Fig. 11) and uninfected (Fig. 12) cell near the gland lumen. Note the differences

in the length of ER cisternae (*Er*), the ribosomes on ER, the Golgi fields (*Gg*) and the amount of secreted granules (*Sg*). *Gl*, gland lumen; *Mv*, microvilli. *Bars* = 1  $\mu$ m

**Fig. 13.** Longitudinal semithin section through a salivary gland, showing an infected cell (*left*) adjacent to an uninfected cell (*right*), separated by the intercellular lumen with saliva. *Gl*, gland lumen. *Bar* = 25  $\mu$ m



chondria are less numerous and many of them are in a stage of progressing disorganization, whereby they are changed into minute vacuoles in which the remains of cristae adhere to the wall. These degradations are the same as those previously observed in sciarids by Jurand et al. (1967); however, as these authors point out, the data are insufficient to enable a discussion as to whether these changes render mitochondria more or less efficient. As seen from the functional aspect, to accomplish its double function of nourishing the parasites and producing saliva, the parasitized cell would need an increased activation of cell functions including its mitochondrial activity. As shown in Fig. 10, the endoplasmic reticulum (ER) of parasitized cells showed a moderate degree of disintegration and ribosomes were often free, not fixed to ER cisternae; moreover, the incidence of pinocytotic vesicles was comparatively high. In non-parasitized cells, the ER was well developed, sometimes occurring in stocks of cisternae with attached ribosomes; vacuoles and smooth ER were rare. Such differences were more pronounced in areas near the gland lumen. Figure 11, a higher magnification of the electron-lucent apical area illustrated in Fig. 13, shows very thin cytoplasm containing only short fragments of ER. Golgi fields can hardly be detected and the dark granules, which apparently contribute to the production of saliva, are scarce. In contrast, a comparable area of the non-parasitized cell (Fig. 12) showed well-developed ER, some Golgi fields, and granules that apparently originated there and migrated to the lumen of the gland. Consequently, as Fig. 13 suggests, the parasitized cell contributes less to the production of saliva, but the latter is not totally inhibited as previously suggested by Keyl (1960).

The first appearance of saliva in intercellular lumina provided with a border of microvilli begins in the third larval instar (Wülker, unpublished data); at this time, parasites are well developed and must therefore have an influence on the accumulation of saliva from the beginning. Destruction of the cytoplasm, depletion of ribosomes from the ER, diminution of the number of Golgi fields, vacuolization and high pinocytotic activity in the parasitized cell have also been found in parasitized cells

of sciarids after microsporidian infection (Jurand et al. 1967).

Therefore, parasitization of different groups of midges by different species of microsporidia cause very similar pathological effects on the salivary glands.

**Acknowledgements.** The authors wish to thank the Øyvind Schnell/Zoological Museum Bergen for valuable help in the collection of infected material and Dr. S. Økland, Zoological Institute, for fixation of the material for electron microscopy. R. Rössler at the University of Freiburg performed the preparation of material for electron microscopy and prepared photographs of the ultrastructure, and Dr. G.A. Schaub gave critical comments to the text. The travel to Bergen was supported by a grant from the University of Freiburg.

## References

- David L (1991) Role of the hemocytes in distribution of microsporidia in the insect body. *J Invertebr Pathol* (in press)
- Jacob J, Jurand A (1965) Electron microscope studies on salivary gland cells: V. The cytoplasm of *Smittia parthenogenetica* (Chironomidae). *J Insect Physiol* 11:1337–1343
- Jurand A, Simoes LCG, Pavan C (1967) Changes in the ultrastructure of the salivary gland cytoplasm in *Sciara ocellaris* (Comstock 1882) due to microsporidian infection. *J Ins Physiol* 13:795–803
- Karnovsky MJ (1965) A formaldehyde-glutaraldehyde fixation of high osmolality for use in electron microscopy. *J Cell Biol* 27:137A–138A
- Keyl H-G (1960) Erhöhung der chromosomalen Replikationsrate durch Mikrosporidieninfektion in Speicheldrüsenzellen von *Chironomus*. *Naturwissenschaften* 47:212–213
- Keyl H-G (1963) Veränderungen der DNS-Verteilungsverhältnisse in Speicheldrüsenchromosomen während der Replikation. *Zool Anz [Suppl]* 27:78–84
- Kloetzel JA, Laufer H (1969) A fine-structural analysis of larval salivary gland function in *Chironomus thummi* (Diptera). *J Ultrastruct Res* 29:15–36
- Larsson R (1982) Cytology and taxonomy of *Helmichia aggregata* gen. et spec.nov. (Microspora, Thelohaniidae) a parasite of *Endochironomus* larvae (Diptera, Chironomidae). *Protistologica* 18:355–370
- Wülker W (1987) Effects of a microsporidian infection in the salivary gland of *Chironomus* larvae (Diptera) [Abstract]. *Zentralbl Bakteriol Mikrobiol [A]* 265:536